

## Polarization reversal and jump-like domain wall motion in stoichiometric LiTaO<sub>3</sub> produced by vapor transport equilibration

V. Ya. Shur, A. R. Akhmatkhanov, I. S. Baturin, and E. V. Shishkina

Citation: [Journal of Applied Physics](#) **111**, 014101 (2012); doi: 10.1063/1.3673601

View online: <http://dx.doi.org/10.1063/1.3673601>

View Table of Contents: <http://scitation.aip.org/content/aip/journal/jap/111/1?ver=pdfcov>

Published by the [AIP Publishing](#)

---

### Articles you may be interested in

[Polarization reversal and domain kinetics in magnesium doped stoichiometric lithium tantalate](#)

Appl. Phys. Lett. **105**, 152905 (2014); 10.1063/1.4898348

[Investigation of the nanodomain structure formation by piezoelectric force microscopy and Raman confocal microscopy in LiNbO<sub>3</sub> and LiTaO<sub>3</sub> crystals](#)

J. Appl. Phys. **110**, 052013 (2011); 10.1063/1.3623778

[Thermal stability of Li Ta O 3 domains engineered by scanning force microscopy](#)

Appl. Phys. Lett. **89**, 142906 (2006); 10.1063/1.2357556

[Domain reversal in stoichiometric LiTaO 3 prepared by vapor transport equilibration](#)

Appl. Phys. Lett. **85**, 4445 (2004); 10.1063/1.1814436

[Wall velocities, switching times, and the stabilization mechanism of 180° domains in congruent LiTaO 3 crystals](#)

J. Appl. Phys. **83**, 941 (1998); 10.1063/1.366782

---

A promotional banner for the Journal of Applied Physics. It features the AIP logo and the journal title at the top. Below this, the text 'Meet The New Deputy Editors' is centered. At the bottom, there are three circular headshots of the new deputy editors, each with their name written to the right: Christian Brosseau, Laurie McNeil, and Simon Phillpot. The background is a vibrant orange with a pattern of small, colorful dots.

# Polarization reversal and jump-like domain wall motion in stoichiometric $\text{LiTaO}_3$ produced by vapor transport equilibration

V. Ya. Shur,<sup>a)</sup> A. R. Akhmatkhanov, I. S. Baturin, and E. V. Shishkina*Ferroelectric Laboratory, Research Institute of Physics and Applied Mathematics, Institute of Natural Sciences, Ural Federal University, Ekaterinburg 620000, Russia*

(Received 9 November 2011; accepted 1 December 2011; published online 4 January 2012)

The polarization reversal and domain structure evolution has been studied in stoichiometric lithium tantalate prepared by vapor transport equilibration process. The first *in situ* visualization of domain kinetics has demonstrated the jump-like motion of few strictly oriented plane domain walls, which leads to short isolated current pulses in the switching current data. The proposed model of jump-like domain wall motion caused by interaction with pinning centers representing the areas with increased value of the threshold field is based on the effect of retardation of bulk screening. The derived formulas were applied successfully for analysis of the field dependence of the total switching time. The durations of wall jumps and wall stays (rest times) extracted from the switching current data are analyzed separately. The deceleration of the wall motion velocity during jump is controlled by the trail of residual depolarization field produced by bound charges and screening charges in the area behind the wall. The duration of the rest time is governed by the bulk screening of residual depolarization field. The value of Hurst exponent 0.75 obtained by fractal analysis of the switching current data has confirmed the essential influence of prehistory on the domain wall motion. The measurements of the coercive field by switching in bipolar triangular pulses in wide range of the field ramp rate have allowed us to extract the record low value of coercive field 60 V/mm for quasi-static polarization reversal. © 2012 American Institute of Physics. [doi:10.1063/1.3673601]

## I. INTRODUCTION

The nonlinear-optical ferroelectric crystals with engineered periodic domain structure are applied for efficient frequency conversion based on quasi-phase-matching effect.<sup>1,2</sup> The periodically poled lithium niobate  $\text{LiNbO}_3$  (LN) single crystal is the most popular material for such applications, due to its high nonlinear optical coefficients and availability of high-quality wafers. The second harmonic generation by usual congruent LN crystals is limited. Doping of LN crystals by MgO allows to solve the problem partially, but the needs of industry require further increase of the average and peak powers of second harmonic generation. The recently demonstrated achievements on this way are associated with utilization of lithium tantalate  $\text{LiTaO}_3$  (LT) single crystals.<sup>3</sup>

LT single crystals are typically grown by Czochralsky method from a congruently melting composition. Congruent lithium tantalate (CLT) crystals possess essential deviation from the stoichiometric composition with the Li deficiency (ratio  $[\text{Li}]/[\text{Li}+\text{Ta}]$  equals to 0.485)<sup>4</sup> and large concentration of point defects (Li vacancies and  $\text{Ta}_{\text{Li}}$  antisites). Two effects, which are associated with antisite point defects,<sup>5–7</sup> limit the maximal input power of coherent light during frequency conversion for LT (so as LN) single crystals: photo refractive damage (PRD) and green-induced infrared absorption (GRIIRA). Extremely high value of coercive field obtained in CLT, which hampers the formation of periodical

domain structures for frequency conversion applications, is also related to nonstoichiometric point defects.<sup>4</sup>

Several methods were applied during the past decades to produce LT and LN crystals with near stoichiometric composition (NSLT and NSLN). The crystals grown by double crucible Czochralsky method (NSLT-CZ)<sup>8</sup> and potassium-flux growth method<sup>9</sup> demonstrate great reduction of point defect concentration. However, both methods are quite challenging to implement, due to precise control of material flux and temperature requirements. Vapor transport equilibration (VTE) is an alternative method based on post-annealing of single crystalline CLT wafers at high temperature for obtaining the near stoichiometric composition (VTE-LT). The method looks essentially simpler than crystal growth methods.<sup>10,11</sup> Annealing of a CLT wafer in a Pt crucible with pre-reacted Li-rich powder of 70%  $\text{LiO}_2$  and 30%  $\text{Ta}_2\text{O}_5$  at temperatures about 1100–1300 °C are used for realization of the VTE process.

The measured value of the  $[\text{Li}]/[\text{Li}+\text{Ta}]$  ratio in VTE-LT wafers is equal to 0.500; therefore, the wafers are essentially closer to stoichiometric composition than grown NSLT crystals.<sup>4</sup> Moreover, VTE-LT wafers demonstrate a record low value of coercive field<sup>12</sup> and essential decrease of PRD and GRIIRA effects.<sup>13</sup> Such improved optical and ferroelectric properties make VTE-LT crystals very promising for production of nonlinear optical devices with tailored domain structure.<sup>14</sup>

The polarization reversal process was studied in VTE-LT crystals by integral methods only.<sup>12,14</sup> The activation-type field dependence of the switching time was revealed.<sup>12</sup>

<sup>a)</sup>Author to whom correspondence should be addressed. Electronic mail: vladimir.shur@usu.ru.

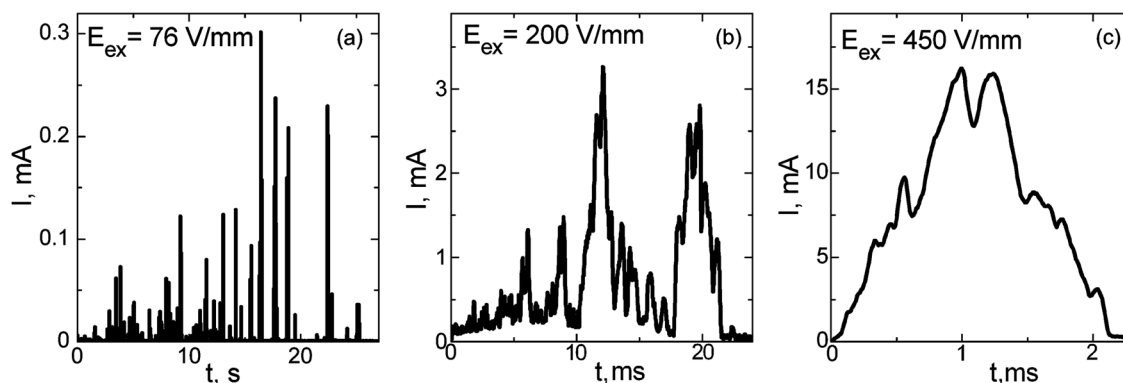


FIG. 1. Switching currents obtained during polarization reversal by rectangular field pulses with various pulse amplitudes. (a) Low-field range; (b) and (c) high-field range.

It was shown that the measured value of coercive field essentially depended on “the period of hysteresis loop”, but no further analysis of obtained dependence was performed.<sup>14</sup> The coercive field value below 100 V/mm was measured. It was pointed out that the direct visualization of the domain kinetics failed due to low contrast of domain walls.<sup>12</sup> Therefore, the field dependence of the domain wall motion velocity was estimated from the switching current analysis only with low reproducibility of obtained results.<sup>14</sup>

The record efficiency of second harmonic generation was demonstrated.<sup>13</sup> The periodically poled VTE-LT crystals allowed to obtain second harmonic generation of a 10 W ( $\lambda = 532 \text{ nm}$ ) continuous wave from 29 W ( $\lambda = 1064 \text{ nm}$ ) radiation in a 4-cm-long device near room temperature.

It leads to the conclusion that the very promising practical results require the systematical investigation of domain kinetics in VTE-LT, including *in situ* observation of the domain structure evolution in the electric field.

## II. EXPERIMENT

Domain kinetics were investigated in Z-cut commercial single crystalline CLT (Crystal Technology, CA), NSLT-CZ (Yamaju Ceramics, Japan), and VTE-LT (Silicon Light Machines, CA). CLT crystals were 0.2 mm thick, NSLT-CZ — 0.9 mm thick, and VTE-LT — 0.8 mm thick.

VTE-LT wafers were produced by vapor transport equilibration process during 100 h at 1100 °C. The typical sample area was about  $20 \times 10 \text{ mm}^2$ .

Most of the results were obtained during application of electric field using liquid electrolyte (saturated LiCl water solution or tap water) electrodes 3–6 mm in diameter formed by a special sample fixture made of Plexiglas with silicone rubber pads. Such a sample fixture allowed *in situ* optical visualization of domain kinetics during application of electric field both in transmission and reflection modes. The field ramp rate dependence of the coercive field was also measured using DC ion plasma sputtered solid electrodes: metal (100-nm-thick Ni) and conductive oxide (200-nm-thick  $\text{In}_2\text{O}_3:\text{Sn}$  (ITO)). The similar electrodes of 2–3 mm in diameter were deposited on both polar sides of the wafer. All switching experiments were performed at room temperature.

Programmable, arbitrary-shaped voltage signals were generated by a NI PCI-6251 multifunctional data acquisition board, amplified by high-voltage amplifier TREK 20/20 C, and applied to the electrodes. A precision resistor (0.2, 2, 20, or 200 k $\Omega$ , depending on current range) connected in series with the sample was used for recording of the switching current. The switching charge was obtained by digital integration of the switching current data. The switching area was supposed to be equal to the electrode area.

Triangular and rectangular switching field pulses were used. The triangular ones allowed obtainment of the hysteresis loop. Rectangular pulses were used for investigation of the switching current and for *in situ* visualization of the domain kinetics.

Domain kinetics was observed *in situ* by polarized microscope Carl Zeiss LMA 10 in transmission mode and recorded by digital video camera with simultaneous recording of the switching current. A high resolution (1.3 MPix) digital video camera with frame rate up to 15 fps was used. The images of the static domain structure were also taken by an Olympus BX51 optical microscope in transmission, reflection, phase contrast, and dark field modes.

## III. SWITCHING BY RECTANGULAR PULSES

### A. Switching current shapes

Detailed analysis of the switching current parameters recorded during application of the rectangular electric field pulses has been performed. Field rise time (0.1 ms) is chosen to be essentially shorter than minimal observed switching time (about several milliseconds). The amplitude of applied external field  $E_{ex}$  ranged from 70 to 500 V/mm. The upper limit is caused by the current limit of the high-voltage amplifier (20 mA), while, below 70 V/mm, the noise hampers the current measurements.

The switching current shape qualitatively changes while increasing the applied field (Fig. 1). At low-field range below 140 V/mm, one can obtain the set of isolated short current pulses (Fig. 1(a)). It must be noted that the duration of individual pulses is in millisecond range, whereas the total switching time, representing the time interval from the beginning to the end of the polarization reversal, is about tens



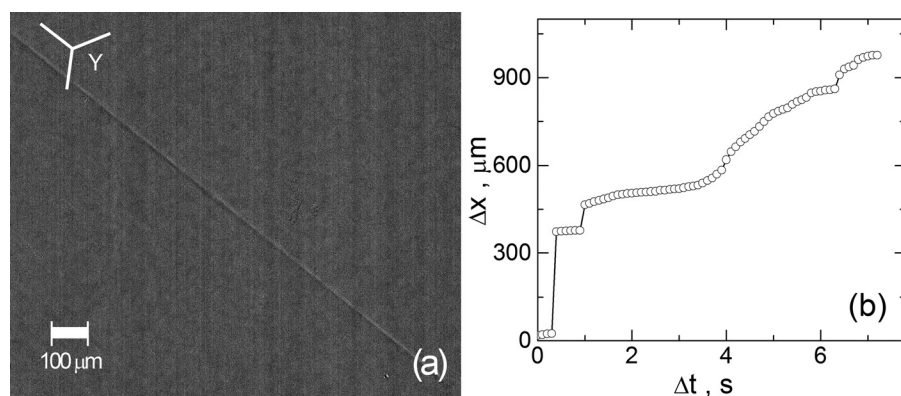


FIG. 2. (a) The instantaneous image of the moving domain wall in VTE-LT after image processing. (b) The extracted time dependence of wall position.  $E_{ex} = 90$  V/mm.

of seconds. The averaged period of the pulses is about 100 ms, and the summarized duration of individual pulses is about one percent from the total switching time.

The averaged period of the pulses rapidly decreases with field growth. In the high-field range (above 140 V/mm), the continuous current with strong modulation of the current amplitude (noise component) was obtained during the whole switching process (Figs. 1(b) and 1(c)). A similar switching current shape was observed in NSLT.<sup>15</sup>

*In situ* observation of the domain structure evolution in congruent LN allowed us to attribute the isolated current pulses to individual jumps of the domain walls.<sup>16</sup> Nevertheless, the direct observation of the domain kinetics in VTE-LT had never been reported.

## B. Domain kinetics

We have studied the evolution of the domain structure in VTE-LT by optical microscopy during polarization reversal. The chosen pulse amplitude 90 V/mm results in the switching time of about 10 seconds, which is long enough to record the domain kinetics with sufficient time resolution. It was mentioned earlier that relatively low applied field (two orders of magnitude lower, as compared to CLT) led to small electro-optically induced change of refractive index and to very weak contrast of the domain walls in VTE-LT single crystals.<sup>12,17</sup> As a result, all previous attempts to visualize the domain kinetics in VTE-LT were unsuccessful.<sup>12</sup>

In our experiments, the contrast of domain walls is increased by special image processing of recorded video sequences. We have averaged several images without domain walls captured before the starting of the switching process. The resulting background image is subtracted from each subsequent instantaneous image of domain structure

evolution. Such procedure and contrast enhancement allow us to visualize the moving domain walls.

It has been shown that the domain kinetics in VTE-LT is similar to kinetics earlier observed in NSLT-CZ.<sup>15</sup> Polarization reversal process from the single-domain state starts with the appearance of a few hexagonal domains with Y-oriented domain walls at the electrode edge. The subsequent domain kinetics evolves through jump-like motion of oriented domain walls (Fig. 2(a)). The small number of the moving domain walls allows us to separate out and to analyze the motion of the single domain wall. The time dependence of the wall position revealed by image analysis (Fig. 2(b)) allows us to obtain the sideways wall motion velocity. For example, the averaged domain wall velocity equal to 0.14 mm/s and peak domain wall velocity equal to 3.5 mm/s have been obtained for pulse amplitude 90 V/mm. It should be noted that the revealed peak value of the wall velocity is reduced, due to limited time resolution of the video camera.

Let us compare the obtained behavior of the domain structure with domain kinetics in CLT. The main features of domain evolution in CLT are as follows:<sup>15</sup> (1) the high density of nucleation centers up to  $1000 \text{ mm}^{-2}$  (Fig. 3(a)); (2) triangular shape of growing isolated domains with domain walls oriented along X crystallographic directions; (3) the intensive merging of growing domains; and (4) smooth shape of the switching current. Two clearly distinguishable domain growth mechanisms have been obtained: (1) slow growth of isolated domains (Fig. 3(a)) and (2) fast wall motion after domain merging (Figs. 3(b) and 3(c)). Thus, the domain kinetics in VTE-LT differs drastically from CLT.<sup>18</sup> Comparison of the main features of domain kinetics in CLT and VTE-LT can be seen in Table I.

It is necessary to point out that, in VTE-LT, the continuous wall motion with varying velocity has been observed in

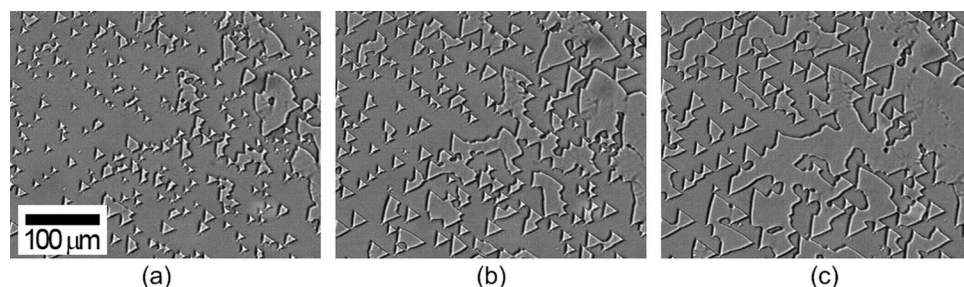


FIG. 3. Instantaneous images of domain structure evolution in CLT with time intervals 100 ms.  $E_{ex} = 21$  kV/mm.

TABLE I. Comparison of domain kinetics in CLT and VTE-LT.

	CLT	VTE-LT (in low fields)
Coercive field	About 21 000 V/mm	About 60 V/mm
Density of nuclei	About 1000 mm <sup>-2</sup>	About 1 mm <sup>-2</sup>
Domain shape	Triangular	Hexagonal
Orientation of domain walls	Along X-crystallographic axis	Along Y-crystallographic axis
Mechanism of domain kinetics	Merging of growing domains	Jump-like wall motion
Switching current	Smooth shape	Set of individual short pulses

the high field region only, whereas, in low fields (below 140 V/mm), the jump-like motion appears and, during the main part of the switching process, the wall does not move.

The obtained behavior can be explained while taking into account the wall interaction with the pinning centers (defects). We suppose that the studied VTE-LT wafers contain the local regions with threshold field values above the average level. The experimental field dependence of the sideways domain wall motion velocity in LN and LT crystals in low field range (just above threshold field) is approximated usually by the following equation:

$$v(E_{ex}) = \mu(E_{ex} - E_{th}), \quad (1)$$

where  $\mu$  is the wall mobility,  $E_{ex}$  is the applied field, and  $E_{th}$  is the threshold field.

The wall motion process represents generation of the steps at the existing domain wall (2D nucleation) and step growth along the wall (1D nucleation). In the uniaxial crystal, the nucleation probabilities of both processes are defined by the local value of the polar component of electric field averaged over the volume of nucleus (switching field).<sup>19,20</sup> We have proposed a mechanism of the jump-like (jerky) domain wall motion. It is known that the domain wall decelerates after shifting from the initial position. This effect is due to reduction of the switching field at the wall by residual depolarization field ( $E_{rd}$ ) produced by bound charges and screening charges in the area behind the wall.<sup>21</sup> It is necessary to take into account that  $E_{rd}$  appears due to retardation of the bulk screening process. We suppose that, after long enough time, the complete screening occurs with full compensation of depolarization field by slow bulk screening.<sup>22</sup>

The decrease of the switching field during the shift of the domain wall from the initial position is caused by formation of the trail of the depolarization field produced by bound charges, which change the sign as a result of reorientation of the spontaneous polarization behind the wall and are mainly compensated by the fast external screening process. The external screening in the wafer with electrodes on the polar surfaces is very fast (time constant is about hundreds of microseconds); however, the existence of the intrinsic surface dielectric layer leads to incomplete external screening.<sup>19</sup> Thus, it is possible to take into consideration only the residual depolarization field  $E_{rd} = E_{dep} - E_{ext,scr}$ , which can be compensated by slow bulk screening processes only.<sup>23</sup>

The measured bulk screening time constants vary essentially in the LT family from a few seconds in CLT to 50 ms in NSLT-CZ.<sup>15</sup> It must be pointed out that complete screen-

ing needs much longer time and relaxation processes can be revealed even in hours and days after polarization reversal.<sup>24</sup>

The domain wall starts to move from the initial position if the switching pulse amplitude is above the threshold value. The wall motion velocity  $v$  gradually decreases with shift from the initial position, due to increase of  $E_{rd}$  produced by the trail. The dependence of  $E_{rd}$  on the shift value  $\Delta x$  for the plane domain wall can be written as follows:<sup>25</sup>

$$E_{rd}(\Delta x) = P_s L / (d \varepsilon_L \varepsilon_o) F(\Delta x / d), \quad (2)$$

where  $F(\Delta x / d) = 1 / \pi [2 \arctg(\Delta x / d) + \Delta x / d \ln(1 + d^2 / \Delta x^2)]$ ,  $d$  is the sample thickness,  $L$  and  $\varepsilon_L$  are the thickness and dielectric constant of the surface dielectric layer, respectively,  $P_s$  is the spontaneous polarization, and  $\varepsilon_o$  is the permittivity of vacuum.

Thus, the field dependence of the domain wall motion velocity can be written as

$$v(E_s(\Delta x, x, t)) = \mu[E_s(\Delta x, t) - E_{th,loc}(x)] \quad (3)$$

with the following dependence of the local value of the switching field on time and shift:

$$E_s(\Delta x, t) = E_{ex} - [E_{rd}(\Delta x) - E_b(t)], \quad (4)$$

where  $E_b(t)$  is the bulk screening field and  $E_{th,loc}(x)$  is the maximal local value of the threshold field along the wall for a given wall position.

The threshold field value in any real crystal is spatially nonuniform, and the areas with locally increased  $E_{th,loc}$  can play the role of the pinning centers (defects). The domain wall stops when  $E_s(\Delta x, t) < E_{th,loc}(x)$ . During stay ("rest time"),  $E_s(\Delta x, t)$  increases, due to compensation of  $E_{rd}$  by bulk screening, and the domain wall restarts when  $E_s(\Delta x, t) > E_{th,loc}(x)$ . The wall stops at the next pinning center. Thus, in low applied fields just above  $E_{th}$ , the wall motion represents fast jumps between pinning centers with comparatively long rest times (stays at pinning centers) (Fig. 4).

It was shown experimentally that the duration of each wall jump was much shorter than the bulk screening time constant.<sup>15</sup> Therefore, the decreasing of  $E_{rd}$  is obtained during rest time only. The distance between the pinning centers and the pinning strength (excess of  $E_{th,loc}$  on the pinning center over the average value) defines the duration of the rest time.

### C. Field dependence of the switching time

The recording of the switching current has been used for obtaining the field dependence of the switching time, which

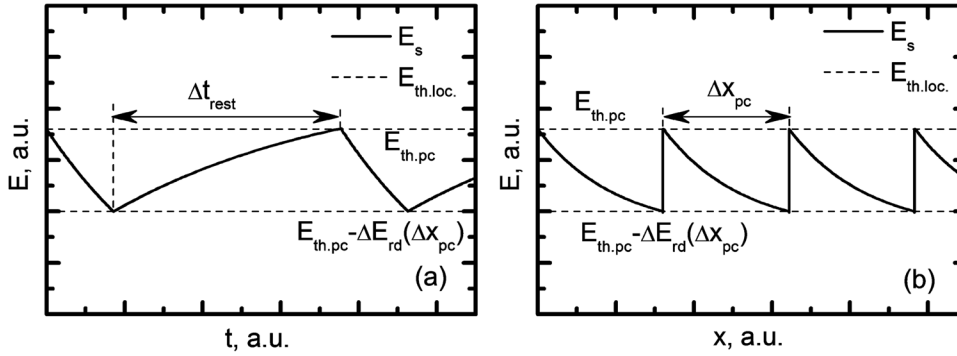


FIG. 4. The switching field dependences during jump-like motion: (a) on time and (b) on domain wall position.

is the classical characteristic of the polarization reversal process (Fig. 5).<sup>26</sup> The switching time value has been extracted from the time dependence of the switched charge  $Q_s(t)$  and defined as the time required for switching of 0.95 of the total  $Q_s$ .

For explanation of the obtained data in the wide range of the switching times (Fig. 5), it is necessary to take into account the qualitative difference of the domain kinetics in low and high fields.

**In the high-field range** (above 140 V/mm), the wall motion is continuous (“nonstop”). The switching time is defined by the wall motion velocity, which has been approximated by the activation type field dependence in this field range. The measured field dependence of the switching time (Fig. 5) has been fitted by the following formula:

$$t_s(E_{ex}) = t_0 \exp[E_{ac}/(E_{ex} + E_{int})], \quad (5)$$

where  $E_{ac}$  is the activation field,  $E_{int}$  is the internal bias field, and  $t_0$  is the time constant.

The revealed values are  $E_{ac} = 915 \pm 15$  V/mm and  $E_{int} = 2$  V/mm. It is worth noting that the obtained value of the internal bias field  $E_{int}$  is several orders of magnitude lower than the lowest applied field, which complicates its measurement by this method.

**In the low-field range** (below 140 V/mm), the jump-like wall motion takes place and the domain wall stays the most time of the switching process. Therefore, a qualitatively different model based on the key role of the bulk screening retardation has to be considered for explanation of  $t_s(E_{ex})$ . Let

us consider the simplified model for the jump-like motion of a single plane domain wall in the ferroelectric crystal with regularly distributed pinning centers, which corresponds to the constant length of the wall jumps ( $\Delta x_{pc}$ ). Let us characterize all pinning centers by equal value of the local threshold field  $E_{th.pc}$ .

For steady wall motion (Fig. 4), the value of  $E_s$  at the moment when the domain wall restarts from the pinning center after staying during the time interval  $\Delta t_{rest}$  can be obtained from the following relation:

$$E_s(\Delta x_{pc}, \Delta t_{rest}) = E_{th.pc}, \quad (6)$$

which can be rewritten in the following form:

$$E_{ex} - [E_{rd}(\Delta x_{pc}) - E_b(\Delta t_{rest})] = E_{th.pc}. \quad (7)$$

The chosen time dependence of the bulk screening field  $E_b(t)$  was experimentally obtained for CLT and NSLT-CZ:<sup>27</sup>

$$E_b(t) = E_{rd}(\Delta x_{pc}) \{1 - \exp[-(t/\tau)^\beta]\}, \quad (8)$$

where  $\tau$  is the bulk screening time constant and  $\beta$  is an exponent.

Finally, the following equation has been obtained for the field dependence of the domain wall rest time:

$$\Delta t_{rest}(E_{ex}) = \tau \{-\ln[(E_{ex} - E_{th.pc})/(E_{ex} - E_{th.pc} + \Delta E_{rd}(\Delta x_{pc}))]\}^{1/\beta}, \quad (9)$$

where  $\Delta E_{rd}(\Delta x_{pc})$  is the increase of  $E_{rd}$  as a result of the wall jump.

In the low-field range, the field dependence of the total switching time according to the discussed simplified model is equal to

$$t_s(E_{ex}) = N_j \Delta t_{rest}(E_{ex}), \quad (10)$$

where  $N_j$  is the number of the wall jumps, which is independent on the field value.

Equation (10) has been used for fitting of the experimental data in the field range below 140 V/mm (Fig. 5). The values of the exponent  $\beta$  and  $E_{th.pc}$  are fixed during fitting. The exponent value equal to 0.3 is chosen according to our earlier experimental results.<sup>28</sup> The value of  $E_{th.pc}$  equal to 60 V/mm is chosen as the lowest external field in which polarization

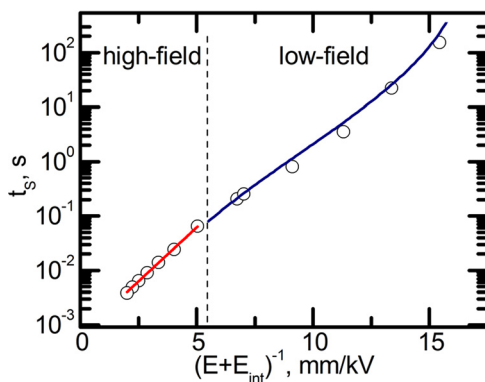


FIG. 5. (Color online) Dependence of the total switching time on external field fitted by Eq. (10) in low-field range and by Eq. (5) in high-field range.

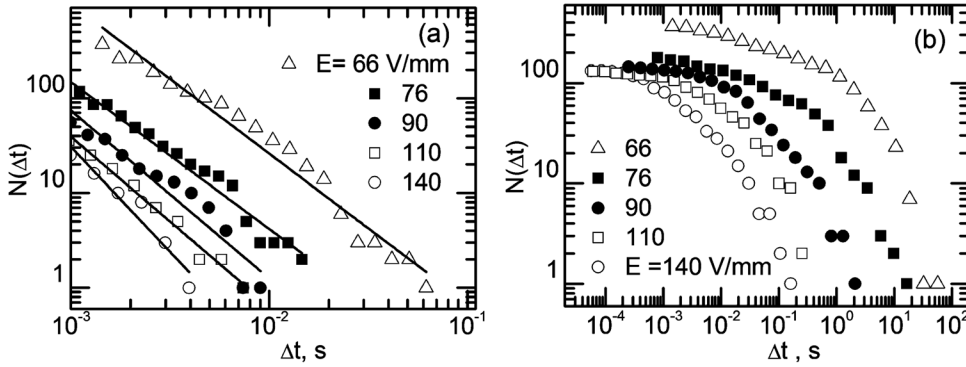


FIG. 6. Cumulative distribution functions for (a) wall jump time and (b) rest time.

reversal started in our study. The number of wall jumps  $N_j = 73$  corresponds to the averaged experimentally observed value.

The fitting of  $t_s(E_{ex})$  data has allowed us to reveal the values of the bulk screening time constant ( $\tau = 670 \pm 70$  ms) and the averaged increase of the residual depolarization field as a result of wall jump ( $\Delta E_{rd}(\Delta x_{pc}) = 19 \pm 1$  V/mm). The more detailed study of the jump-like domain wall motion in ferroelectrics will be presented by us elsewhere.

#### D. Statistical analysis of the switching current

The switching current data was analyzed by the statistical methods developed for the noise signals and fractal records in time.<sup>29</sup> The treatment of the current data by modified Korcak method<sup>30</sup> allows us to separate the cumulative distribution functions for the current pulse width and for the rest time. We have analyzed independently the intervals below the given current level (duration of the domain wall jumps) and above this level (duration of the domain wall stay) for the data recorded in the field range from 60 to 140 V/mm, in which the switching current represents the number of distinguished individual short pulses.

We have analyzed the current pulses with width ranged from 1 to 100 ms. The obtained cumulative statistics for domain wall jump time  $N(\Delta t)$  (number of the current pulses with width above the given value  $\Delta t$ ) is approximated by the following formula:

$$N(\Delta t) = B \Delta t^{-\alpha}, \quad (11)$$

where  $\alpha$  is the exponent and  $B$  is the constant.

It has been shown that the exponent value equal to  $1.59 \pm 0.06$  (Fig. 6(a)) is almost independent of the applied

field value. It is known that the observed scale invariance is typical for self-assembled processes.<sup>29</sup> The constancy of the current pulse (wall jumps) number in the whole field range demonstrates that the moving domain wall interacted with the same set of pinning centers.

For statistical analysis of the rest time data (Fig. 6(b)), the power law dependence with exponential cutoff has been applied, because the self-similar behavior occurs in the finite time range only,

$$N(\Delta t) = B \Delta t^{-\alpha} \exp(-\Delta t/\xi), \quad (12)$$

where  $\xi$  is the fractal correlation time.

The field dependences of the fitting parameters  $\alpha$  and  $\xi$  are presented in Fig. 7.

The Hurst exponent ( $H$ ) extracted by classical Korcak method<sup>30</sup> is equal to  $0.75 \pm 0.01$ , which is the clear evidence of the persistent process with long-time correlation. In other words, it demonstrates the dependence of the domain wall kinetics on prehistory. This fact confirms the proposed model based on the influence of the long-time bulk screening processes on the wall motion. The comparison of the obtained Hurst exponent value, with one revealed for NSLT-CZ ( $H = 0.70 \pm 0.05$ ), demonstrates that, in VTE-LT, the memory effects are more pronounced.

#### IV. SWITCHING IN TRIANGULAR PULSES

We have studied the dependence of the switching process in VTE-LT in linearly increasing alternating field on the field ramp rate  $R = dE/dt$  by recording the switching current data during application of bipolar triangular field pulses with varying period and constant amplitude. The value of  $R$  has

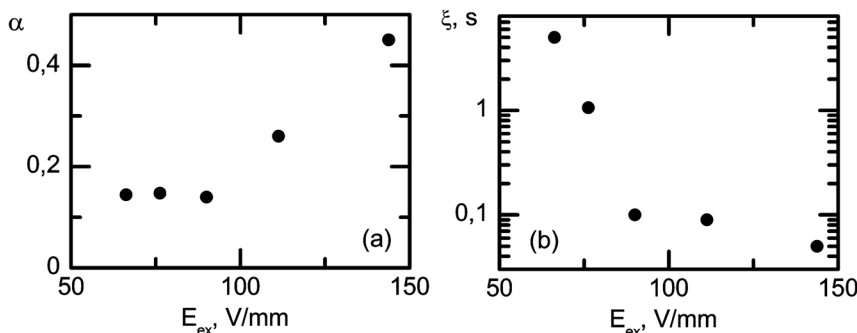


FIG. 7. Dependence on pulse amplitude of fitting parameters (a)  $\alpha$  and (b)  $\xi$  of cumulative distribution functions for rest time.



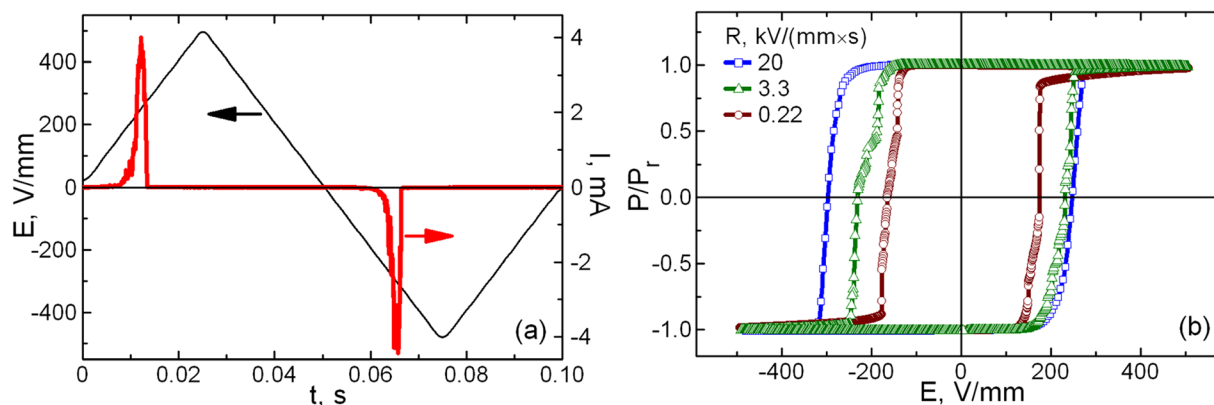


FIG. 8. (Color online) (a) Time dependence of applied external field and switching current in VTE-LT during switching in triangular field pulses. (b) Hysteresis loops recorded for various field ramp rates.

ranged from 20 to 20 000 V/(mm·s), corresponding to pulse frequency from 0.01 to 10 Hz and pulse amplitude 500 V/mm. Such conditions allow us to obtain the complete switching in the whole frequency range. The typical switching current shapes and hysteresis loops for various values of  $R$  are presented in Fig. 8. It is seen that the coercive field  $E_c$  essentially depends on  $R$ .

The obtained dependence of the coercive field on the external field ramp rate (Fig. 9) is approximated by the power law proposed by Ishibashi *et al.*,<sup>31,32</sup>

$$E_c(R) = E_c^0 + AR^\gamma, \quad (13)$$

where  $E_c^0$ ,  $A$ , and  $\gamma$  are the fitting parameters.

The value of exponent  $\gamma$  is found to be equal to 0.18. Such approximation allows us to estimate the limit value of coercive field  $E_c^0$  for quasi-static polarization reversal, corresponding to  $R$  tends to zero  $E_c^0 = 60$  V/mm. This record low value of the coercive field for crystals of the LT and LN family confirms the high quality of the investigated crystals.

The influence of the electrode material on  $E_c$  has been also studied. It is shown that the measured value of  $E_c$  for ITO electrodes is about 10% lower than that for liquid electrodes (Fig. 9).

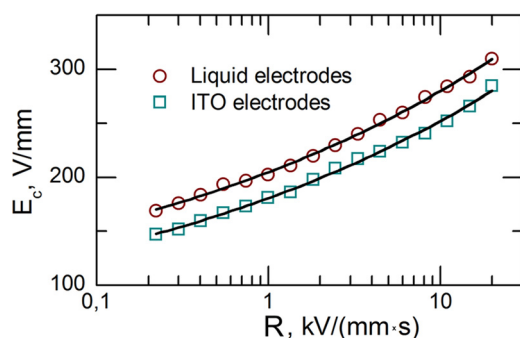


FIG. 9. (Color online) Dependence of coercive field on field ramp rate in VTE-LT fitted by Eq. (13).

## V. CONCLUSION

The domain kinetics during polarization reversal has been studied in stoichiometric lithium tantalate single crystals prepared from congruent composition by the vapor transport equilibration process (VTE-LT). The first *in situ* visualization of domain kinetics in VTE-LT using special image processing has allowed us to reveal the jump-like motion of few Y-oriented plane domain walls. The switching current data consisting of short isolated current pulses has been statistically analyzed by separation of the jump times and the rest times. The model of domain wall motion in ferroelectric with pinning centers representing the areas with increased value of the threshold field has been proposed. The key role of the retardation of the bulk screening of the depolarization field has been considered. The derived theoretical formulas have been used for fitting the field dependence of the total switching time. The fractal analysis of the switching current data has demonstrated the influence of prehistory on the domain wall kinetics, thus confirming the proposed model of the wall motion based on the influence of the long-time bulk screening processes on switching kinetics. The value of the coercive field for quasi-static polarization reversal has been obtained by approximation of the experimental data measured in wide range of the field ramp rate. Thus, it has been shown that the VTE process allows us to obtain a record low value of coercive field 60 V/mm.

## ACKNOWLEDGMENTS

The authors would like to acknowledge R. Route, D. Hum, L.L. Galambos, and R.O. Miles for providing samples of VTE-LT. The research was made possible in part by RFBR (Grants 10-02-96042-r-Ural-a, 10-02-00627-a, and 11-02-91066-CNRS-a) and by Ministry of Education and Science (Contract 16.552 11 7020).

<sup>1</sup>R. L. Byer, *J. Nonlinear Opt. Phys. Mater.* **6**, 549 (1997).

<sup>2</sup>J. Armstrong, N. Bloembergen, J. Ducuing, and P. Pershan, *Phys. Rev.* **127**, 1918 (1962).

<sup>3</sup>K. Mizuuchi and K. Yamamoto, *Appl. Phys. Lett.* **66**, 2943 (1995).

<sup>4</sup>S. Kim, V. Gopalan, K. Kitamura, and Y. Furukawa, *J. Appl. Phys.* **90**, 2949 (2001).



- <sup>5</sup>M. Jazbinšek, M. Zgonik, S. Takekawa, M. Nakamura, K. Kitamura, and H. Hatano, *Appl. Phys. B* **75**, 891 (2002).
- <sup>6</sup>Y. Furukawa, K. Kitamura, A. Alexandrovski, R. K. Route, M. M. Fejer, and G. Foulon, *Appl. Phys. Lett.* **78**, 1970 (2001).
- <sup>7</sup>K. Kitamura, Y. Furukawa, S. Takekawa, M. Nakamura, A. Alexandrovski, and M. Fejer, in *Conference on Lasers and Electro-Optics Europe - Technical Digest* (IEEE, Baltimore, 2001), pp. 255–256.
- <sup>8</sup>Y. Furukawa, *J. Cryst. Growth* **197**, 889 (1999).
- <sup>9</sup>G. I. Malovichko, V. G. Grachev, E. P. Kokanyan, O. F. Schirmer, K. Betzler, B. Gather, F. Jermann, S. Klauer, U. Schlarb, and M. Wöhlecke, *Appl. Phys. A* **56**, 103 (1993).
- <sup>10</sup>P. F. Bordui, R. G. Norwood, D. H. Jundt, and M. M. Fejer, *J. Appl. Phys.* **71**, 875 (1992).
- <sup>11</sup>P. F. Bordui, R. G. Norwood, C. D. Bird, and J. T. Carella, *J. Appl. Phys.* **78**, 4647 (1995).
- <sup>12</sup>L. Tian, V. Gopalan, and L. Galambos, *Appl. Phys. Lett.* **85**, 4445 (2004).
- <sup>13</sup>M. Katz, R. K. Route, D. S. Hum, K. R. Parameswaran, G. D. Miller, and M. M. Fejer, *Opt. Lett.* **29**, 1775 (2004).
- <sup>14</sup>D. S. Hum, R. K. Route, G. D. Miller, V. Kondilenko, A. Alexandrovski, J. Huang, K. Urbanek, R. L. Byer, and M. M. Fejer, *J. Appl. Phys.* **101**, 93108 (2007).
- <sup>15</sup>V. Ya. Shur, E. V. Nikolaeva, E. I. Shishkin, V. L. Kozhevnikov, A. P. Chernykh, K. Terabe, and K. Kitamura, *Appl. Phys. Lett.* **79**, 3146 (2001).
- <sup>16</sup>I. S. Baturin, M. V. Konev, A. R. Akhmatkhanov, A. I. Lobov, and V. Ya. Shur, *Ferroelectrics* **374**, 136 (2008).
- <sup>17</sup>E. Soergel, *Appl. Phys. B* **81**, 729 (2005).
- <sup>18</sup>V. Ya. Shur, E. V. Nikolaeva, E. I. Shishkin, A. P. Chernykh, K. Terabe, K. Kitamura, H. Ito, and K. Nakamura, *Ferroelectrics* **269**, 195 (2002).
- <sup>19</sup>V. Ya. Shur, *Ferroelectrics* **340**, 3 (2006).
- <sup>20</sup>R. Miller and G. Weinreich, *Phys. Rev.* **117**, 1460 (1960).
- <sup>21</sup>V. Ya. Shur, E. L. Rumyantsev, D. V. Pelegov, V. L. Kozhevnikov, E. V. Nikolaeva, E. L. Shishkin, A. P. Chernykh, and R. K. Ivanov, *Ferroelectrics* **267**, 347 (2002).
- <sup>22</sup>V. Ya. Shur and E. L. Rumyantsev, *Ferroelectrics* **191**, 319 (1997).
- <sup>23</sup>V. Ya. Shur, *J. Mater. Sci.* **41**, 199 (2006).
- <sup>24</sup>V. Ya. Shur, V. V. Letuchev, and I. V. Ovechkina, *Phys. Solid State* **26**, 2091 (1984).
- <sup>25</sup>M. E. Drougard and R. Landauer, *J. Appl. Phys.* **30**, 1663 (1959).
- <sup>26</sup>W. J. Merz, *J. Appl. Phys.* **27**, 938 (1956).
- <sup>27</sup>I. S. Baturin, A. R. Akhmatkhanov, V. Ya. Shur, M. S. Nebogatikov, M. A. Dolbilov, and E. A. Rodina, *Ferroelectrics* **374**, 1 (2008).
- <sup>28</sup>V. Ya. Shur, A. R. Akhmatkhanov, I. S. Baturin, M. S. Nebogatikov, and M. A. Dolbilov, *Phys. Solid State* **52**, 2147 (2010).
- <sup>29</sup>J. Feder, *Fractals* (Plenum, New York, 1988).
- <sup>30</sup>J. Russ, *Fractal Surfaces* (Plenum, New York, 1994).
- <sup>31</sup>S. Hashimoto, H. Orihara, and Y. Ishibashi, *J. Phys. Soc. Jpn.* **63**, 1601 (1994).
- <sup>32</sup>H. Orihara, S. Hashimoto, and Y. Ishibashi, *J. Phys. Soc. Jpn.* **63**, 1031 (1994).